Title: **Fibroblasts as an in vitro model of circadian genetic and genomic studies**

Authors: Marcelo Francia1, Merel Bot2, Toni Boltz3, Juan F. De la Hoz4, Marco Boks5, René Kahn5, Roel Ophoff2

Affiliation: 1. Interdepartmental Program for Neuroscience, David Geffen School of Medicine, University of California Los Angeles, Los Angeles, CA, USA
2. Center for Neurobehavioral Genetics, Semel Institute for Neuroscience and Human Behavior, UCLA
3. Department of Human Genetics, David Geffen School of Medicine, University of California Los Angeles, Los Angeles, CA, USA
4. Bioinformatics Interdepartamental Program, University of California Los Angeles, Los Angeles, CA, USA
5. Brain Center University Medical Center Utrecht, Department Psychiatry, University Utrecht, Utrecht, The Netherlands.

ABSTRACT

Bipolar disorder (BD) is a heritable disorder characterized by shifts in mood that manifest in manic or depressive episodes. Clinical studies have identified abnormalities of the circadian system in BD patients as a hallmark of underlying pathophysiology. Fibroblast cells collected from BD patients show temporal differences in the expression of core circadian genes. We set out to examine the underlying genetic architecture of circadian rhythm in an in vitro fibroblast model, in order to disentangle the polygenic nature of BD disease risk. We collected, from primary cell lines of 6 healthy individuals, temporal genomic features over a 48 hour period from transcriptomic data (RNA-seq) and open chromatin data (ATAC-seq). The RNA-seq data showed that only a limited number of genes, such as *ARNTL*, *CRY1*, *PER3*, *NR1D2* and *TEF* display circadian patterns of expression consistently across cell cultures. The ATAC-seq data identified that distinct transcription factor families, like those with the basic helix-loop-helix motif, were associated with regions that were increasing in accessibility over time. Further evaluation of these regions using stratified linkage disequilibrium score regression (sLDSC) analysis failed to identify a significant presence of them in the known genetic architecture of BD, and other psychiatric disorders or neurobehavioral traits in which the circadian rhythm is affected. This study characterizes the biological pathways that are activated in this in vitro circadian model,

evaluating the relevance of these processes in the context of the genetic architecture of BD and other disorders, highlighting its limitations and future applications for circadian genomic studies.

BACKGROUND

It is estimated that the lifetime worldwide prevalence of bipolar disorder (BD) is 1% (Moreira et al. 2017), with an estimated heritability of 60-85% (Song et al. 2015); (Bienvenu, Davydow, and Kendler 2011). Genome-wide association studies (GWAS) of BD are showing a highly polygenic genetic architecture of disease susceptibility with common genetic variants explaining 20% of the heritability (Stahl et al. 2019); (Mullins et al. 2021). BD is primarily characterized by shifts in mood, which result in manic or depressive episodes. Clinical studies have associated abnormalities of the circadian system in Bipolar disorder type 1 (BD1) patients as a hallmark component of its pathophysiology, with disturbed sleep quality being identified as an early symptom of manic episodes (Leibenluft et al. 1996). Furthermore, dysregulation of sleep and wake cycles during manic episodes include sleep abnormalities such as decrease in total sleep time, delta sleep, and REM latency (Levenson and Frank 2011). These abnormalities have also extended to other circadian regulated systems such as cortisol levels. Multiple studies have found greater morning levels of cortisol in BD outpatients and in non-manic states when compared to controls (Girshkin et al. 2014). Despite these findings, the precise mechanisms of altered circadian rhythms in BD remain unclear.

The circadian rhythms synchronize physiological processes with the environment, creating and maintaining an internal 24 hour cycle. The main controller of the circadian cycle in mammals is the suprachiasmatic nucleus (SCN), a brain region located in the basal hypothalamus. It receives environmental cues, also called zeitgebers, such as light information from the retina which is relayed using synaptic and hormonal signaling (Le Minh et al. 2001) to the rest of the brain and body. At the molecular level, the circadian machinery within every cell (Schibler and Sassone-Corsi 2002) consists of multiple transcriptional feedback loops, where core circadian genes *BMAL1* and *CLOCK* induce the expression of their own repressors, *PER1, PER2, PER3* and *CRY1, CRY2*. These genes modulate different layers of gene expression, from modifying the chromatin landscape to make certain regions of the genome more or less accessible(Menet, Pescatore, and Rosbash 2014), to post-transcriptional modifications altering the function of the associated proteins at specific times during the day (Robles, Humphrey, and Mann 2017). Disruptions in the circadian rhythms have been associated with neuropsychiatric traits, specifically in mood disorders (Walker et al. 2020), however the direct interactions between them are still being studied.

The localization of the SCN makes direct interaction and collection in humans impossible, with researchers instead using peripheral fibroblast cells to study the molecular and genetic components of this system (Yamazaki and Takahashi 2005). These cells receive cortisol as a circadian signal from the SCN, through the hypothalamic-pituitary-adrenal axis (HPA). In order to study circadian rhythms using cell cultures, the cells need to be synchronized. One approach for this is treating the cells with dexamethasone, which elicits rhythm synchronization between the cells in a culture (Yamazaki and Takahashi 2005). Dexamethasone binds to the glucocorticoid receptor, acting on the same pathways through which cortisol regulates circadian rhythms *in vivo*. This synchronization method has been used in conjunction with luciferase bioluminescence reporter assays to study the molecular dynamics of selected circadian genes *in vitro(Nakahata et al. 2006)*. Studies using these systems have been applied to both sleep disorders and BD. Although researchers were able to find differences in the period of expression of circadian genes in sleep disorders (Hida et al. 2017), similar studies using cells derived from BD1 patients were unable to detect significant (S. Yang et al. 2009) or replicable(McCarthy et al. 2013) differences.

Here we examined what aspects of general biology and circadian related genetic regulation this *in vitro* fibroblast model captures and whether these features relate to the genetic architecture of BD susceptibility. For this, we collected longitudinal temporal sequencing data of both gene expression and accessible chromatin regions. The temporal gene expression was used to identify genes that display circadian oscillations and are under glucocorticoid control, as well as genes with distinct temporal patterns representing other biological pathways. The temporal accessible chromatin data was used to identify regions of the genome and associated transcription factor motifs that are implicated in the temporal regulation of gene expression. Finally, we examined whether the genomic regions showing temporal transcriptomic and epigenomic circadian profiles in primary cultures of fibroblasts were enriched in genetic association signals of BD or other related psychiatric and sleep-related phenotypes.

RESULTS

Temporal RNA-seq captures genes with distinct longitudinal expression patterns

Outside of the subset of genes that compose the core circadian transcriptional feedback loop, most rhythmic genes are tissue specific (R. Zhang et al. 2014). We aimed to identify within fibroblasts the overall longitudinal patterns of all the genes that are temporally regulated and classify them based on their temporal features. For this purpose, we collected RNA-seq data

every 4 hours for a 48-hour period, from cell cultures of 6 human primary fibroblasts that were derived from a skin biopsy of subjects with no psychiatric disorders. After quality control, the temporal RNA-seq dataset consisted of n=11,004 genes. We used a cubic spline regression model to identify genes that had a significant effect of time in their expression ((Y. Wang, Ke, and Brown 2003); (Qin and Guo 2006); (Madden et al. 2017)). This approach identified n=2,767 genes with significant evidence (False discovery rate < 0.05) for temporal changes of gene expression levels. To cluster these genes according to distinct temporal patterns we applied the Weighted Gene Co-Expression Network Analysis (WGCNA)(Langfelder and Horvath 2008), which identifies genes with highly correlated expression levels. WGCNA produced 11 modules with eigengene values that captured the principal time patterns present in the expression of these genes (i.e: temporal modules; Supplemental figure 1). Gene ontology (GO) analysis of WGCNA modules with MetaScape (Zhou et al. 2019) highlighted specific cell processes associated with distinct temporal patterns among 11 of these modules. Figure 1 depicts the eigengene values of 4 temporal modules with significant enrichment of GO terms (adjusted by Benjamini-Hochberg method). Genes in the turquoise module, which show a linear decrease in expression over time, had GO terms for supramolecular fiber organization (p value = 1e-15) and mRNA splicing via spliceosome (p value = 2.5e-13). In compasion, genes in the blue module, which show a linear increase in expression, had a GO term for cellular response to hormone stimulus (p value = 1.3e-9) .The genes in the black module, which show an increase in expression that plateaus by time point 16 (28 hours after dexamethasone treatment), were enriched for chromatin organization(p value = 1e-12) and transcription elongation by RNA polymerase II (p value = 7.9e-8) GO terms. The genes in the brown module, which show an expression pattern opposite of the black module, had a GO term for intracellular protein transport (p value = 1e-18). Lastly the purple module, which has genes with a peak expression at time point 12 (24 hours after dexamethasone treatment), had GO terms for cell division (p value = 1e-67) and mitotic cell cycle (p value = 1e-60). The complete results of GO analysis for all the WGCNA modules are available in Supplementary Table 1.

WGCNA results did not yield a module of co-expressed genes with eigengene values representative of oscillating 24 hrs cycles mimicking a circadian rhythm, nor were circadian related functional enrichment of GO terms found in any of the modules. Next we focused on closely inspecting known circadian genes for skin fibroblasts obtained from CircaDB (Pizarro et al. 2013), a gene expression database for circadian genes in different tissues. Out of the 98 circadian genes reported in CircaDB for skin, we identified 34 genes in our dataset with significant changes in expression over time (Figure 2A). Using the circadian detection tools JTK

Cycle (Hughes, Hogenesch, and Kornacker 2010), LS (Glynn, Chen, and Mushegian 2006), ARSER (R. Yang and Su 2010), Metacycle (Wu et al. 2016) and RAIN (Thaben and Westermark 2014), we aimed to detect significant oscillations within these potential circadian genes and the complete temporal RNA-seq dataset. Among these methods, only JTK and ARSER identified significant periodic expression patterns (after Benjamini-Hochberg correction of 0.05) for *NR1D2*, and further only ARSER identified significant oscillations for 73 genes. However, the predicted period differed between the softwares, with JTK predicting a period of 27.6 hours for *NR1D2*, while ARSER predicted 24.7 hours (Supplementary table 2 and supplementary files). Therefore instead of using these circadian detection tools, we applied smoothing-splines mixed effect models using the R package "sme" (Berk 2018) to model the temporal features of these circadian genes (Figure 2B). These models showed that for some of these circadian genes, such as *CRY2* and *NFIL3*, the circadian expression pattern is only present in some of the cell cultures, whereas for genes such as *NR1D2* and *TEF*, the circadian pattern is ubiquitous across cell cultures from different individuals. The fitted models for these circadian genes were then used in time warping analysis to group genes with known expression dynamics (Figure 2C and Supplementary figure 3). From these expression patterns, we identify that *NR1D2* expression follows its inhibition effect on *ARNTL* and *CRY1 (Rijo-Ferreira and Takahashi 2019).* We also see that *PER3* expression follows its inhibition effect with *ARNTL*. However the expected inhibition relationship between *CRY1* and *ARNTL* was not present (Supplemental figure 4).

Figure 1. Eigengene values for RNA-seq modules obtained from WGCNA

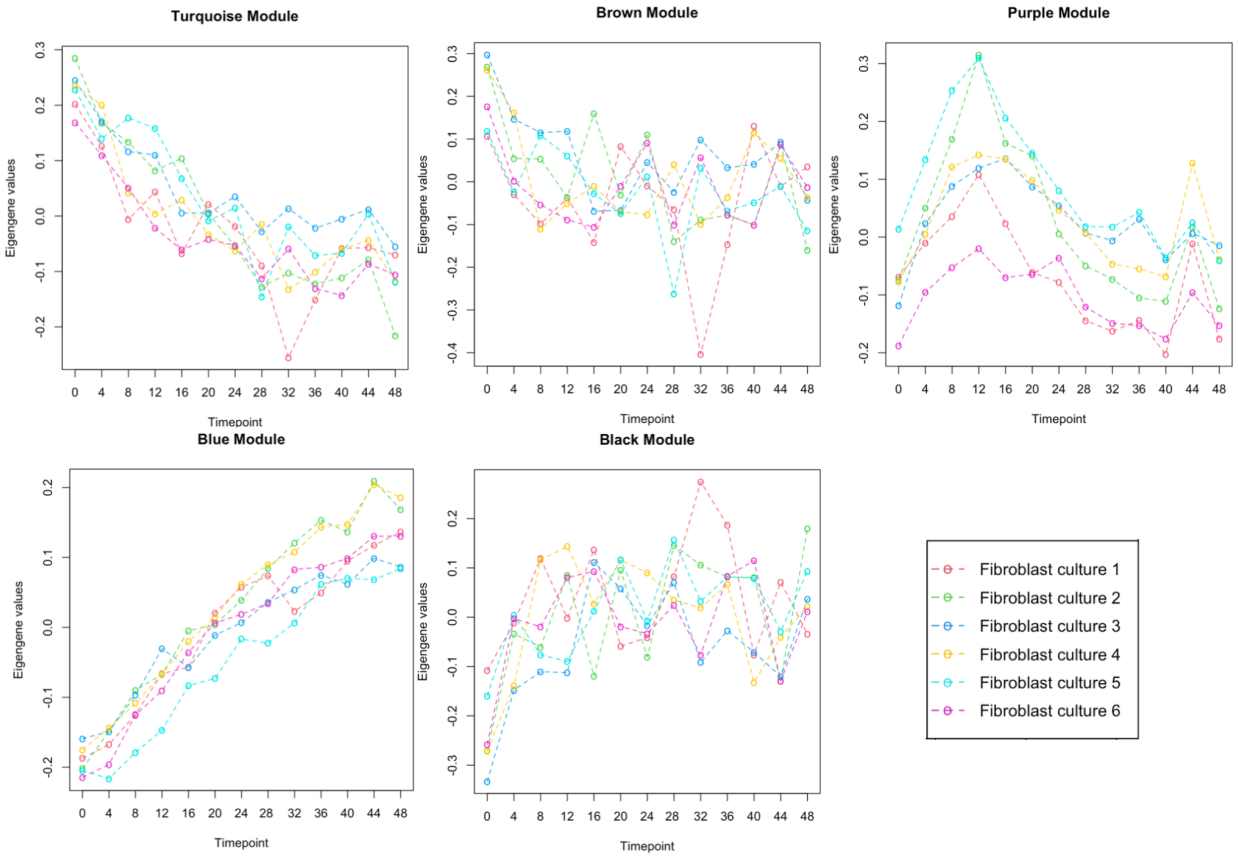

Figure 1 Description: Eigengene modules from WGCNA of the longitudinal temporal expression patterns of RNA-seq data collected every 4 hours for a 48 hour period. Each color represents a fibroblast cell culture from a different individual. The number of genes assigned per module was 505 for Turquoise, 207 for Black, 381 for Brown, and 81 for Purple. Module names were assigned by WGCNA.

Figure 2. Expression patterns and mixed non-linear modeling of circadian genes

A

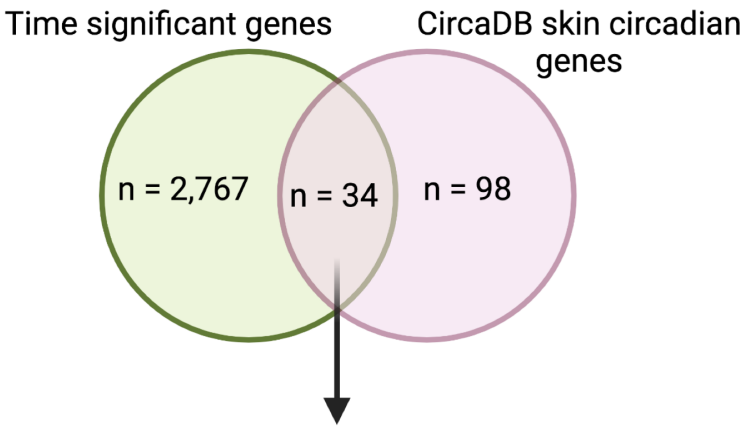

Time significant circadian genes							
NR1D2	FUS	**TEF**	SRPRB	GBP2	SETBP1	HR	**PER3**
ARNTL	KLF9	**DBP**	FDFT1	**CRY1**	VCL	NFIL3	KLF7
KIF7	KIF20A	PIK3IP1	CRY2	B4GALT2	**CDC25B**	ETV5	SLC6A6
FKBP5	F3	C14ORF1	MTHFD2	THAP11	**NPAS2**	THRA	CASP1
STOM	**TRIM5**	PER1					

B

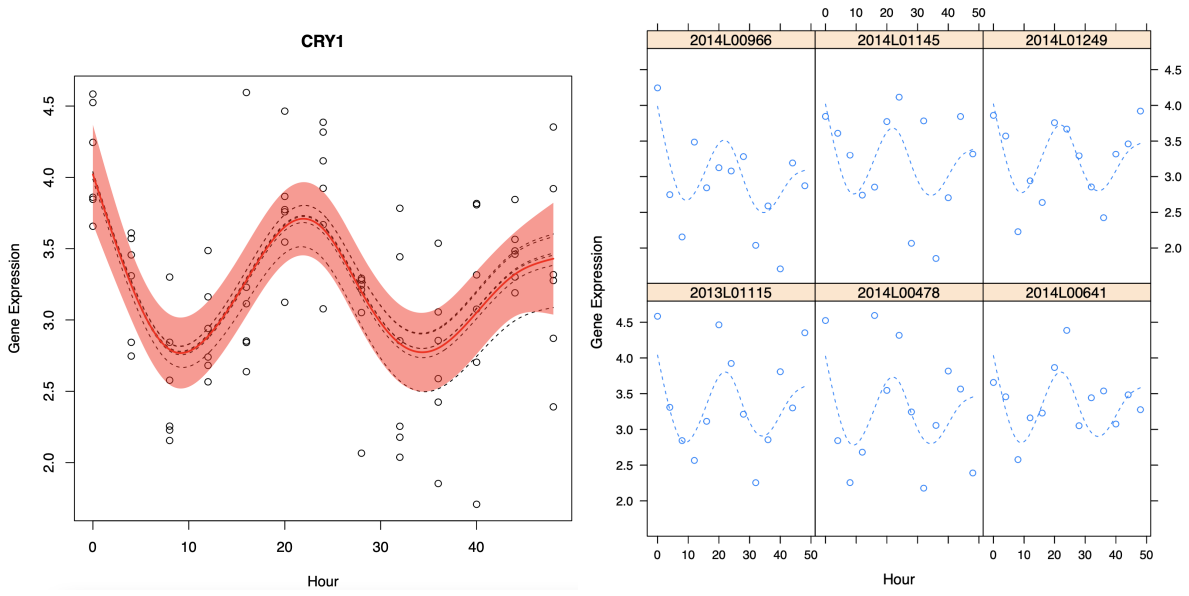

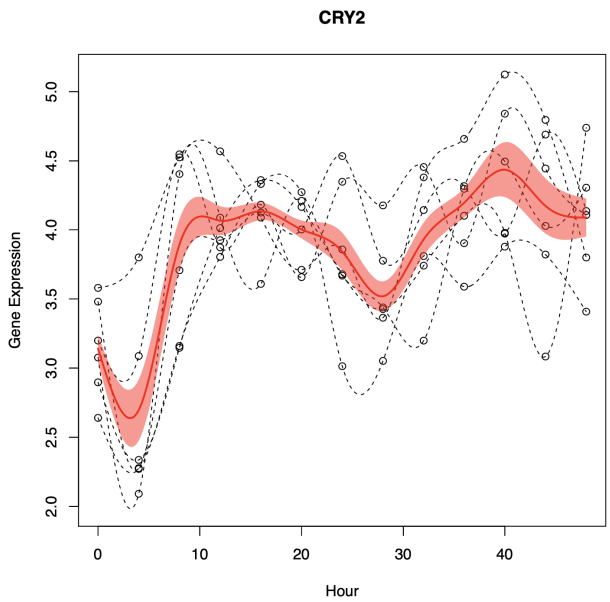
CRY2
Gene Expression
Hour

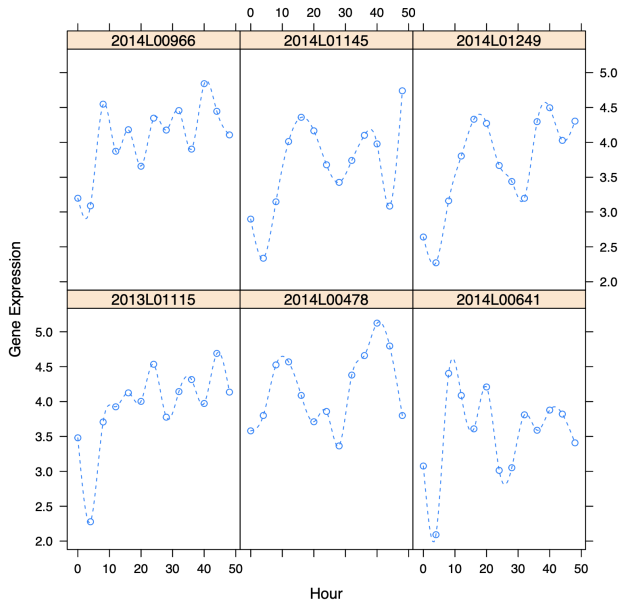
2014L00966
2014L01145
2014L01249
2013L01115
2014L00478
2014L00641
Gene Expression
Hour

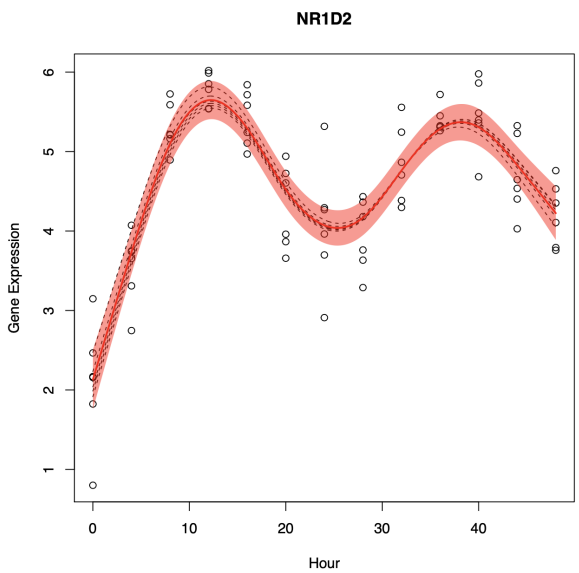
NR1D2
Gene Expression
Hour

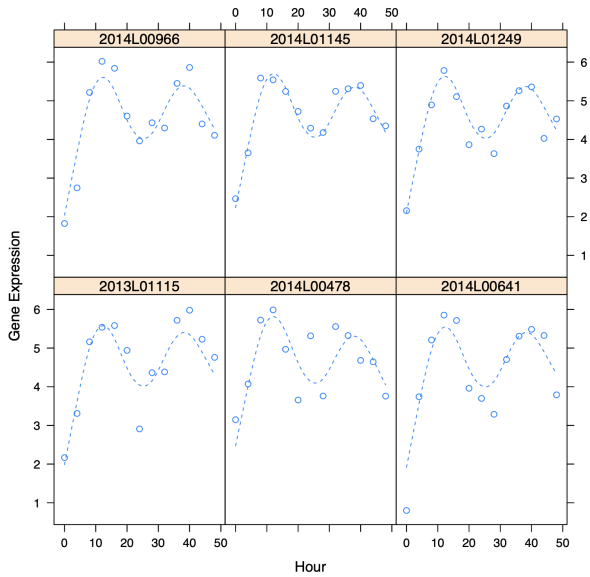
2014L00966
2014L01145
2014L01249
2013L01115
2014L00478
2014L00641
Gene Expression
Hour

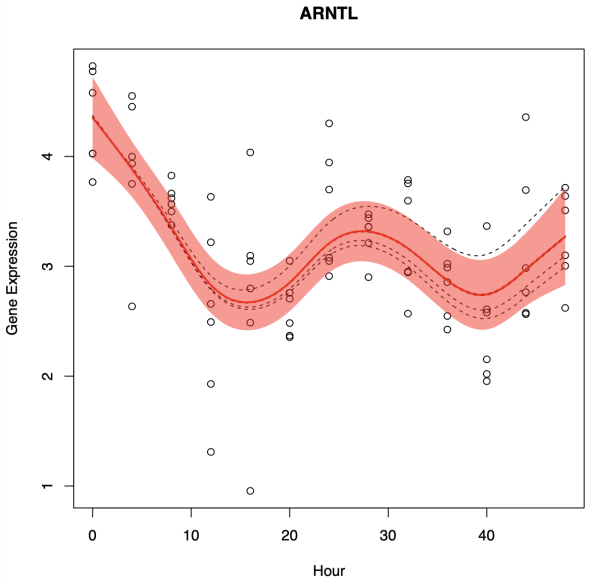
ARNTL
Gene Expression
Hour

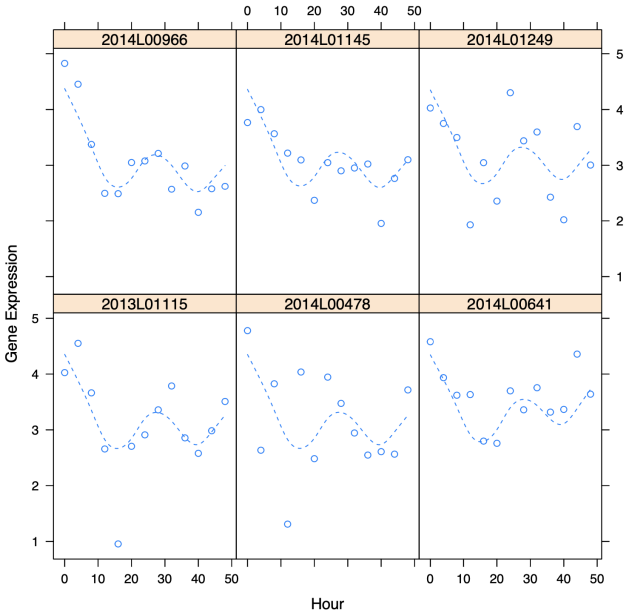
2014L00966
2014L01145
2014L01249
2013L01115
2014L00478
2014L00641
Gene Expression
Hour

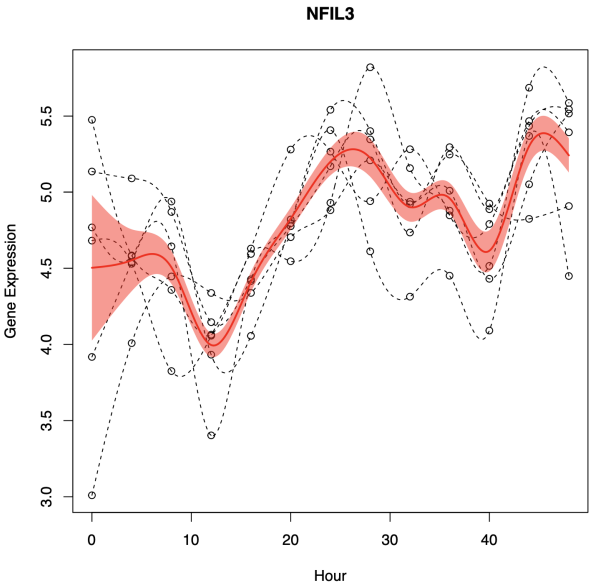
NFIL3
Gene Expression
Hour

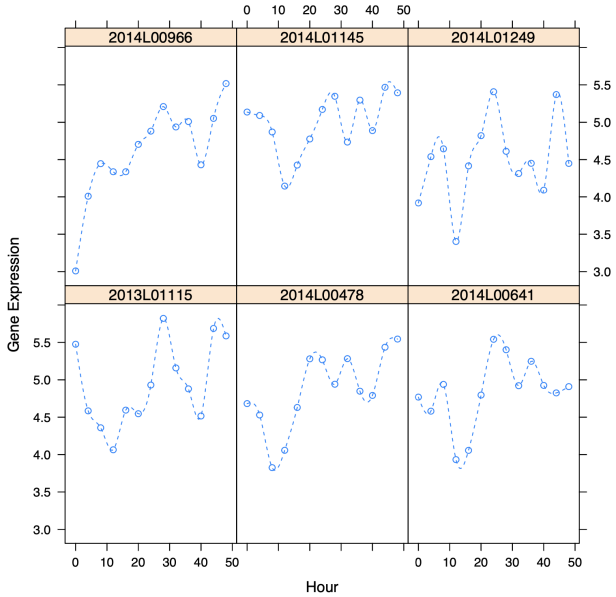
2014L00966
2014L01145
2014L01249
2013L01115
2014L00478
2014L00641
Gene Expression
Hour

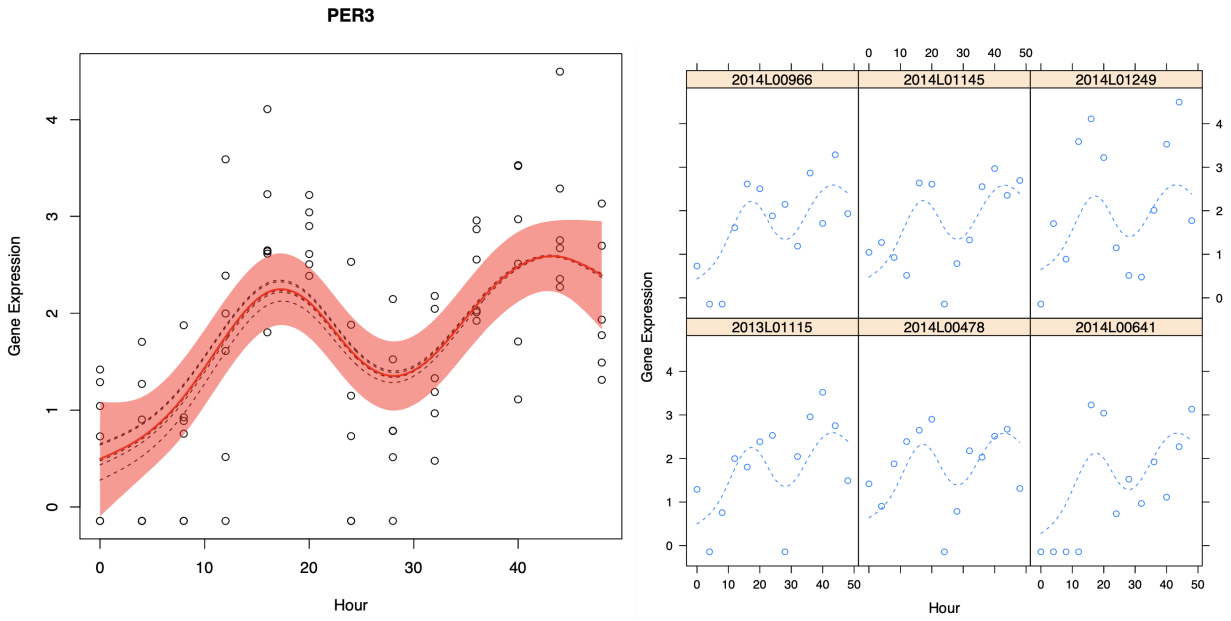

C

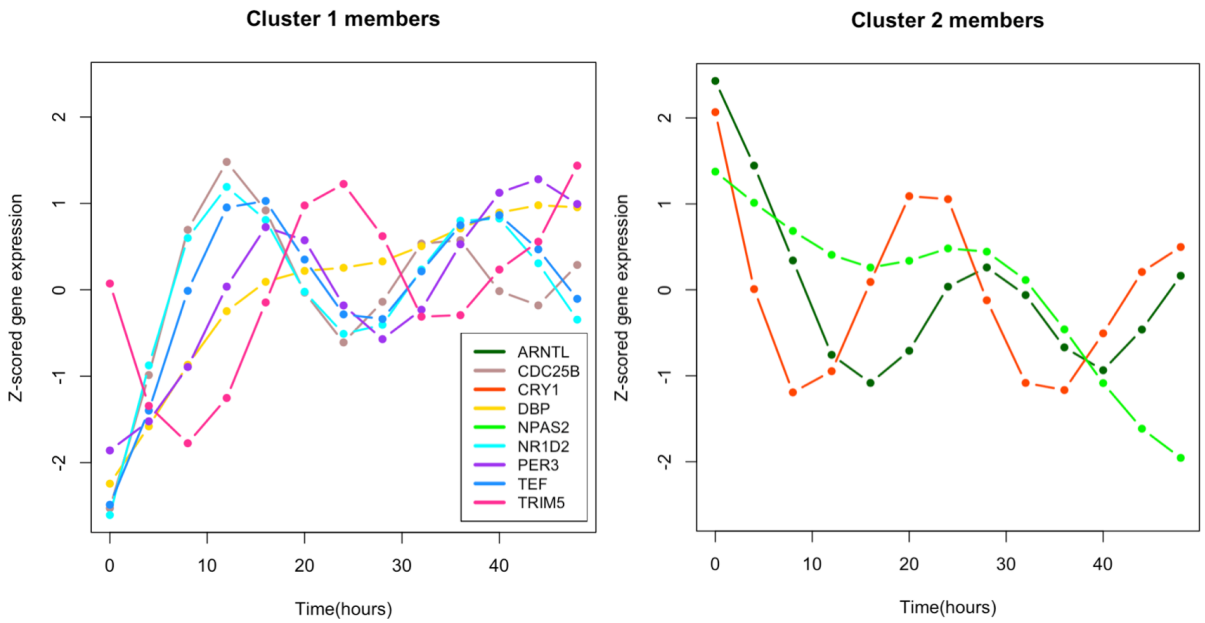

Figure 2 Description A. Overlap of the genes that were found to have a significant effect of time in their expression as well as being previously identified as circadian within the skin tissue. In bold are those genes that displayed expression patterns consistent with circadian rhythms. B. Smoothing-splines mixed-effect model of the genes that displayed circadian oscillations and their known redundant gene partners. The red area indicates the 95 percent confidence interval. Gene expression values are presented as lCPM (log of counts per million) C. Dynamic time warp clustering results of the 9 circadian genes identified in this *in vitro* model. Due to the

differences in magnitude of gene expression across circadian genes, expression values were z-scored.

Temporal open chromatin levels measured by ATAC-seq highlights potential regulatory regions and transcription factor binding sites

To identify regions of the genome associated with the regulation and downstream effects of circadian genes, we collected ATAC-seq data following the same temporal design as with the RNA-seq dataset. Across samples and time points, we merged all overlapping regions of open chromatin, also known as peaks, as described previously (Keele et al. 2020) to define a common set of ATAC-seq signals. We then used cubic spline regression models to identify peaks that have a significant change in accessibility over time. This approach yielded n=7568 time significant peaks, which were functionally annotated using ChipSeeker (Yu, Wang, and He 2015), a software that annotates peaks with the nearest gene and genomic regions. Distributions of genomic functional annotations of these regions are provided in supplementary figure 6B. These peaks with significant changes in accessibility over time showed a similar genomic distribution as the full dataset, as shown in supplementary figure 6A. Following the approach for the RNA-seq data, we applied WGCNA to cluster time significant peaks with similar temporal patterns of accessibility changes (Supplementary figure 5). WGCNA modules of these regions mainly displayed linear patterns of increasing or decreasing ATAC-seq signal over time.

We used HOMER (Heinz et al. 2010), a software toolset that was developed for analyzing Chromatin Immunoprecipitation Sequencing (ChIP-Seq) data, and its applications have been extended to ATAC-seq as well (Yan et al. 2020), to identify enriched motif sequences in chromatin regions with similar temporal patterns. WGCNA identified 15 different modules for the temporal patterns of chromatin accessibility, however the main pattern that characterizes these modules is an overall increase or decrease in accessibility. By analyzing together all the regions that follow similar patterns we had n=3,132 regions increasing in accessibility and n=4,422 decreasing in accessibility. Regions that were decreasing in accessibility over time (Figure 3A) had motif sequences for Fos (p value = 1e-1055), Fra1 (p value = 1e-1049), ATF3 (p value = 1e-1039), BATF (p value = 1e-1004), Fra2 (p value = 1e-1003), AP-1 (p value = 1e-978), Fosl2 (p value = 1e-836), Jun-AP1 (p value = 1e-681), Bach2 (p value = 1e-337) and JunB (p value = 1e-1007). Most of these transcription factors are part of the AP-1 transcription complex. Regions that were increasing in accessibility over time (Figure 3B) had motif sequences for BHLHA15 (p value = 1e-198), TCF4 (p value = 1e-181), NeuroG2 (p value =

1e-161), Twist2 (log p value = 1e-160), Pitx1 (p value = 1e-178), Atoh1 (p value = 1e-167), Tcf21(p value = 1e-150), Olig2 (p value = 1e-134), ZBTB18 (p value = 1e-139) and NeuroD1 (p value = 1e-125). These are dimerizing transcription factors that have the basic helix-loop-helix protein structural motif. In both types of regions HOMER identified the binding sequence of the glucocorticoid response element. For the known circadian transcription factors, HOMER identified significant enrichment of the binding sequences for BMAL1 (p value = 1e-29), NPAS2 (p value = 1e-10), CLOCK (log p value = 1e-9), particularly within regions that had increasing accessibility over time. For the regions with decreasing accessibility over time, HOMER identified enrichment of NFIL3 (p value = 1e-14) and ReverB (p value = 1e-3).

Figure 3 Motif enrichment analysis of time significant peak regions

A

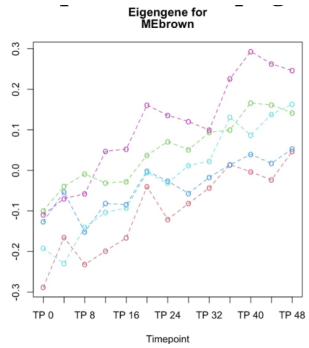

Rank	Motif	Motif Name	P-value	% of Target Sequences with Motif(of 784)	% of Background Sequences with Motif(of 48625)
1		BHLHA15(bHLH)/NIH3T3-BHLHB8.HA-ChIP-Seq(GSE119782)	1E-105	69.77	31.58
2		TCF4(bHLH)/SHSY5Y-TCF4-ChIP-Seq(GSE96915)	1E-99	72.07	34.7
3		NeuroG2(bHLH)/Fibroblast-NeuroG2-ChIP-Seq(GSE75910)	1E-91	71.43	35.64
4		Twist2(bHLH)/Myoblast-Twist2.Ty1-ChIP-Seq(GSE127998)	1E-86	73.47	38.67
5		Pitx1:Ebox(Homeobox,bHLH)/Hindlimb-Pitx1-ChIP-Seq(GSE41591)	1E-85	30.1	6.77
6		Atoh1(bHLH)/Cerebellum-Atoh1-ChIP-Seq(GSE22111)	1E-82	57.02	24.61
7		Tcf21(bHLH)/ArterySmoothMuscle-Tcf21-ChIP-Seq(GSE61369)	1E-77	51.79	21.31
8		Olig2(bHLH)/Neuron-Olig2-ChIP-Seq(GSE30882)	1E-66	75.38	44.92

Open chromatin regions increasing in accessibility					
Rank	Motif Name	Consensus	Log P-value	% of Target Sequences with Motif(of 2707)	% of Background Sequences with Motif(of 46871)
1	BHLHA15(bHLH)		-4.56E+02	62.02%	33.68%
2	TCF4(bHLH)		-4.17E+02	63.72%	36.45%
3	Pitx1:Ebox(Homeobox,bHLH)		-4.12E+02	21.65%	5.47%
4	Atoh1(bHLH)		-3.86E+02	52.20%	27.04%
5	NeuroG2(bHLH)		-3.71E+02	62.73%	36.97%
6	Twist2(bHLH)		-3.69E+02	66.49%	40.72%
7	Tcf21(bHLH)		-3.48E+02	47.10%	23.91%
8	ZBTB18(Zf)		-3.22E+02	31.33%	12.73%
9	Olig2(bHLH)		-3.10E+02	68.01%	44.38%
10	NeuroD1(bHLH)		-2.89E+02	40.64%	20.44%
36	BMAL1(bHLH)		-6.77E+01	47.36%	36.67%
92	NPAS2(bHLH)		-2.32E+01	28.15%	22.85%
94	CLOCK(bHLH)		-2.30E+01	14.26%	10.34%
165	GRE(NR),IR3		-1.18E+01	7.02%	5.08%

B

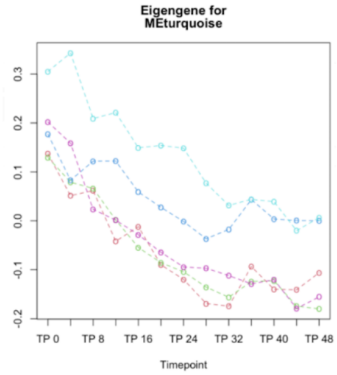

Rank	Motif	Motif Name	P-value	% of Target Sequences with Motif(of 1823)	% of Background Sequences with Motif(of 47840)
1		Fos(bZIP)/TSC-Fos-ChIP-Seq(GSE110950)	1E-641	71.48	14.91
2		Fra1(bZIP)/BT549-Fra1-ChIP-Seq(GSE46166)	1E-626	69.17	14.00
3		Atf3(bZIP)/GBM-ATF3-ChIP-Seq(GSE33912)	1E-621	73.12	16.52
4		JunB(bZIP)/DendriticCells-Junb-ChIP-Seq(GSE36099)	1E-617	67.80	13.47
5		BATF(bZIP)/Th17-BATF-ChIP-Seq(GSE39756)	1E-614	72.30	16.23
6		Fra2(bZIP)/Striatum-Fra2-ChIP-Seq(GSE43429)	1E-613	63.80	11.44
7		AP-1(bZIP)/ThioMac-PU.1-ChIP-Seq(GSE21512)	1E-610	75.26	18.30
8		Fosl2(bZIP)/3T3L1-Fosl2-ChIP-Seq(GSE56872)	1E-488	48.71	7.41

Open chromatin regions decreasing in accessibility					
Rank	Motif Name	Consensus	Log P-value	% of Target Sequences with Motif (of 3650)	% of Background Sequences with Motif (of 46199)
1	Fos(bZIP)		-2.43E+03	67.07%	15.69%
2	Fra1(bZIP)		-2.42E+03	65.32%	14.73%
3	Atf3(bZIP)		-2.39E+03	69.32%	17.39%
4	JunB(bZIP)		-2.32E+03	63.29%	14.20%
5	BATF(bZIP)		-2.31E+03	68.27%	17.33%
6	Fra2(bZIP)		-2.31E+03	59.15%	11.97%
7	AP-1(bZIP)		-2.25E+03	70.14%	19.06%
8	Fosl2(bZIP)		-1.93E+03	45.48%	7.59%
9	Jun-AP1(bZIP)		-1.57E+03	35.26%	5.19%
10	Bach2(bZIP)		-7.77E+02	22.79%	4.36%
58	NFIL3(bZIP)		-3.35E+01	23.62%	18.43%
67	GRE(NR),IR3		-2.78E+01	4.68%	2.61%
78	GRE(NR),IR3		-2.52E+01	7.97%	5.31%
183	Reverb(NR),DR2		-8.70E+00	3.34%	2.38%

Figure 3 description: Motif enrichment analysis results after combining all open chromatin regions that followed a similar change in accessibility over time, including the top 10 motifs as well as motifs associated with circadian genes and glucocorticoid response. P-values were confirmed as significant after Benjamini adjustment cutoff of 1% FDR. A. Eigengene values for the brown WGCNA module and motif enrichment analysis of the associated peak regions, including HOMER results for all peak regions increasing in accessibility. B. Eigengene values for the turquoise module and motif enrichment analysis of the associated peak regions, including HOMER results for all peak regions decreasing in accessibility.

Stratified Linkage Disequilibrium Score Regression(sLDSC) analysis

To examine whether these open chromatin regions highlighted in our study are enriched for genetic susceptibility of BD and other neuropsychiatric traits, we used sLDSC (stratified linkage disequilibrium analysis)(Finucane et al. 2015) to calculate the partitioned heritability of these features. For this approach we used published Psychiatric Genomics Consortium (PGC) summary statistics for BD (Mullins et al. 2021), ADHD (Attention-Deficit/HyperactivityDisorder) (Demontis et al. 2019), schizophrenia (Trubetskoy et al. 2022), PTSD (Post-traumatic stress disorder) (Nievergelt et al. 2019), MDD (Major depression disorder) (Howard et al. 2019), insomnia (Watanabe et al. 2022), and the circadian trait of morningness (Jones et al. 2016). We used the temporally significant ATAC-seq regions with 1 kilobases (kb) and 10 kb genomic windows in both downstream and upstream directions for each region. These ATAC-seq defined annotations were tested jointly with the baseline annotations included with sLDSC (Finucane et al. 2015). Figure 4 shows the enrichment for the traits tested from the ATAC-seq regions annotations as well as the baseline annotations (Full enrichment results are provided in the Supplementary Material). Among these, only the ATAC-seq regions that were decreasing in accessibility had a nominally significant (p value = 4.63e-3) less than expected presence for ADHD, and this effect was not present when the regions are extended by either 1kb or 10kb. In comparison, baseline annotations such as conserved regions in mammals showed a significant enrichment for all the traits (ADHD p value = 7.88e-11, schizophrenia p value = 1.67e-23, BD p value = 1.14e-8, MDD p value = 5.92e-22, insomnia p value = 2.65e-15, morningness p value = 3.05e-29), except PTSD (p value = 0.073). No significant enrichment was observed for the ATAC-seq regions in the other traits that were tested, indicating that these genomic annotations are not contributing to their known genetic architecture.

Figure 4 sLDSC enrichment results for psychiatric disorders and a circadian trait

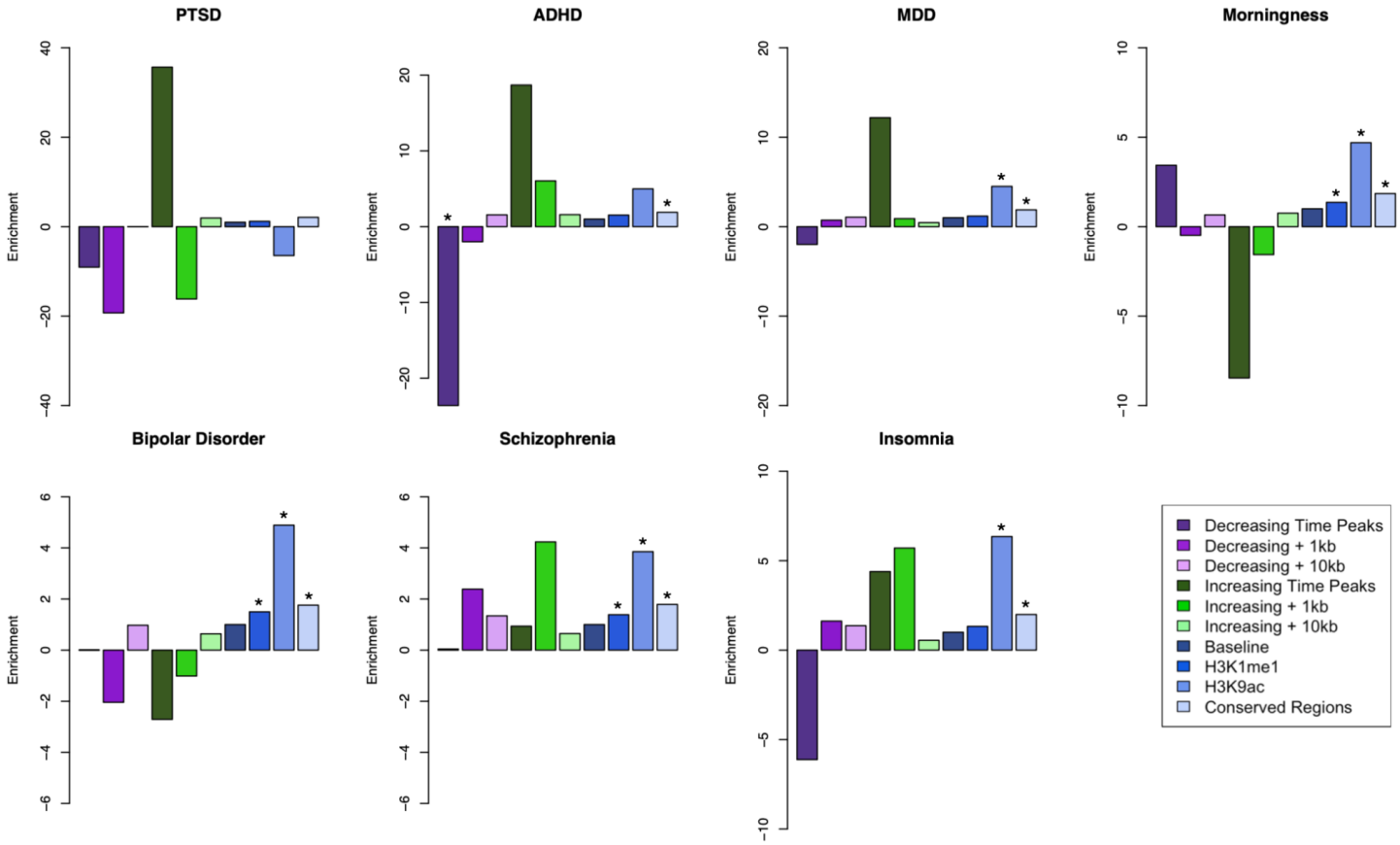

Figure 4 Description: Results of partitioned sLDSC across 3 psychiatric disorders and morningness trait across different genomic annotations. Shown are the enrichment for both the temporal ATAC-seq regions and extended genome windows; as well as annotations part of the baseline model of sLDSC, such as baseline for all the annotations, histone markers H3K9ac, H3K4me1, and conserved regions in mammals. PTSD: Post-traumatic stress disorder; MDD: Major depressive disorder; ADHD: Attention-Deficit / Hyperactivity Disorder. * indicates enrichment p-value below 0.01.

DISCUSSION

Cell cultures of peripheral tissues have been employed as models of *In vitro* circadian clock systems to study their molecular components (Balsalobre, Marcacci, and Schibler 2000) and the disorders in which they are disrupted (Kripke et al. 2009). For this particular model that uses skin fibroblasts, we aimed to characterize the circadian features that are present at gene expression and chromatin accessibility levels, with the goal to identify the circadian genes that are engaged by this system as well as their associated regulatory genomic regions. The gene expression and chromatin accessibility data, due to only having 6 samples, was sparse and had not enough power to get significant associations between them. From the longitudinal RNA-seq data we identified circadian patterns of expression in a limited amount of genes such as *ARNTL, CRY1, PER3, NR1D2 (Rev-erbBeta)* and *TEF*. The mixed linear models showed that for many of these circadian genes, there are noticeable differences in the expression patterns between cell cultures. Only 4 genes, *NR1D2, TEF, PER3* and *DBP* had their fitted models across cell lines within the 95 percent confidence interval, while for 8 genes, *CRY1, ARNTL, NPAS2, PER2, CDC25B* and *TRIM5*, at least one of the cell lines had measurements outside of this confidence interval. Genetic variants have been found to be associated with sleep-wake schedule disorder, delayed phase type, and attention deficit hyperactivity disorder for *CRY1 (Onat et al. 2020)*; atrioventricular septal defect for *NR1D2* (Priest et al. 2016) and advanced sleep phase syndrome 3 for *PER3* (L. Zhang et al. 2016).

When compared to the CircaDB dataset, we identified 37 out of the 98 circadian genes previously identified in this tissue to have a significant effect of time in their expression using cubic spline models. This limited overlap could indicate that this in vitro model is constrained to the circadian genes that are directly activated by a glucocorticoid-like stimulus. Glucocorticoid response elements have been identified for circadian genes such as *PER1, PER2, PER3, CRY1, CRY2, Rev-erbalpha (NR1D1), Rev-erbBeta (NR1D2), DBP, NPAS2* and *BMAL1* (So et al. 2009). Consistent with these results we identified circadian rhythmicity in most of those genes that had previously been identified to have a glucocorticoid response element (GRE), with the exception of *NR1D1*. While we do identify expression levels from *NR1D1*, the lack of a significant circadian oscillation in comparison to the strong results from *NR1D2* could be consistent with their known redundant function for circadian rhythms (Liu et al. 2008). The identification of significant periodic expression patterns for *NR1D2* by JTK and ARSER provides evidence that this gene is displaying circadian expression. However, the differences between the predicted periods indicated that these tools were not best suited for identifying periodicity in this dataset. This could be due to the structure of the temporal RNA-seq data, or a lack of

power. Furthermore, while ARSER identified 73 genes with significant periodic expression patterns, this software is known to have a high false positive rate in high resolution data (Wu et al. 2016). Unexpectedly, while the expression pattern of *CRY1* follows the expected inhibition by *NR1D2* (Chiou et al. 2016), it does not reflect the expected inhibitory action on *ARNTL*, nor the similar phase pattern with its heterodimer partner *PER3*. For the relationship with *PER3*, *CRY1* has been previously reported to have a known phase delay with the *PER* genes (*PER1,2,3*)(Fustin et al. 2009), which could be attributed to the multiple binding sites that *CRY1* has for different circadian modulators, resulting in stimulus and tissue specific temporal dynamics. Based on the time patterns, changes in the expression of *CRY1* appear to precede the expression of *ARNTL* by 4 to 8 hours. This inconsistency at the transcriptional level could indicate that these temporal dynamics might not be directly reflected at the transcriptional level, but rather at the post translational stage. It is worth noting that while *PER2* was not part of the circadian genes reported in CircaDB, we were able to identify patterns that resemble circadian rhythms, indicating that this *in vitro* setting could be eliciting circadian responses that are not present within the skin. One explanation for this could be that in the context of an organism there are multiple signaling pathways acting on a tissue, and while in the absence of these signals, such as in this *in vitro* setting, different pathways may be activated. This would be consistent with the known flexibility and redundancy in function that the core circadian genes possess. Another possibility is that the pathway that activates PER2 is usually inhibited by other signals in the skin, but such signals could be absent in this *in vitro* model.

The longitudinal ATAC-seq data identified regions with significant changes in their accessibility over time that indicate potential regulatory regions in these cell lines, but not in an oscillatory way. Motif enrichment analysis by HOMER of peaks that shared temporal features showed that distinct transcription factor families were associated with the longitudinal increase or decrease in accessibility. Specifically, peaks that were increasing in accessibility over time contained the motif for the basic helix-loop-helix, a structural protein family that includes core circadian genes like *ARNTL* and *CLOCK (Z. Wang et al. 2013)*. For the peaks that were decreasing in accessibility, we identified transcription factor motifs that belonged to the AP-1 transcriptional complex, with further gene ontology analysis of these transcription factors highlighting processes such as response to glucocorticoids. These results indicate that genomic regions with similar changes in accessibility over time could be involved in overlapping biological processes. Further validation experiments are needed to assess how they are implicated in the regulation of the nearby genes, as well as the directionality of this interaction. An additional aspect that we wanted to characterize within this *in vitro* model was the cyclic

binding patterns of circadian genes that act as transcription factors, however we were unable to identify such temporal features in this ATAC-seq dataset. This could be due to differences in how the data was generated, as studies that report cyclic binding have used targeted platforms for transcription factors such as ChIP-seq (Rijo-Ferreira and Takahashi 2019). Furthermore, approaches such as transcription factor footprinting to identify these cyclic binding sites could not be implemented due to the recommended sequencing depth for applying this method to ATAC-seq data is around 200M reads (Yan et al. 2020), while the average sequencing depth for the samples used in this project was around 50M reads.

The partitioned stratified LD score regression analysis mainly showed a significant deflation for the chromatin regions that were decreasing in accessibility over time with ADHD. Although not significant, it mirrored the enrichment for the regions that were increasing in accessibility. When expanding the genomic regions by either 1kb or 10kb both the magnitude and the significance of the enrichment are lost, indicating that this effect could be highly localized for these regions. For the other traits that we examined, the enrichment from the ATAC-seq regions were also attenuated when the genomic region was extended. These results show that these regions are not a relevant component for these neuropsychiatric traits, however the attenuation of the deflation by expanding the genomic window does indicate that the sequences that they contain are specific to those genomic positions. The lack of an overlap between the temporal regulatory regions identified in this study and the known genetic architecture of BD could indicate four different interpretations. First, although peripheral tissues capture the genome of an individual, they don't recapitulate brain molecular physiology, the main tissue implicated in the pathophysiology of BD. Second, it could be that the disruptions in the circadian rhythm are not under strong genetic control and are actually influenced by other downstream processes, such as post-translational modifications and differences at the protein level. Third, the specific circadian pathways that are engaged in this *in vitro* model by dexamethasone (i.e: glucocorticoids) are not part of the genetic architecture of BD. This however does not exclude other circadian pathways that could be engaged by a different synchronizing stimulus. Similar studies that have used serum instead of dexamethasone as a synchronizing agent have identified, aside from the core circadian genes, different sets of circadian genes (Balsalobre, Damiola, and Schibler 1998), (Iyer et al. 1999). Furthermore, there are other stimuli that also act in different ways with the circadian system, such as temperature. Whereas dexamethasone acts through binding of the glucocorticoid receptor, temperature affects heat-shock proteins (Saini et al. 2012). Lastly, the disrupted circadian phenotype is not a constant but rather an episodic state in BD patients. This could indicate that rather than the

regular circadian system being affected by BD, it is the ability to deal with circadian stressors and disruptors that could be affected.

With the knowledge of the specific features that this *in vitro* model is able to capture of the circadian system, we advise care when interpreting the results of such experiments, since they may be heavily influenced by the circadian cycle synchronization method. This can lead to a narrow scope to study the circadian rhythms in the context of neuropsychiatric traits. While the biology that this model captures after circadian synchronization induced by dexamethasone treatment does not seem to be directly involved in the known genetic architecture of BD, this model can still be applied to scientific questions that cannot be explored directly in human subjects. One of the aspects of the dysregulated circadian phenotype in BD patients is that it's an episodic event, rather than an static state of the subjects. This model could be used to characterize the specific biological pathways that are engaged during circadian distress. Furthermore, we can directly compare the responses to circadian distress using fibroblast cell lines derived from BD patients and healthy subjects. Additionally, the accessibility that this *in vitro* model provides could be used to study the effect of lithium, a drug used for treating BD, during such circadian distress.

ACKNOWLEDGMENTS

We would like to acknowledge the advice and expertise of Christopher Colwell for this project, and to Annet van Bergen for their work in collecting the tissue samples used in this study.

MATERIALS AND METHODS

Cell lines and Culture

Fibroblasts were isolated by taking skin biopsies from the nether region. Fibroblast cultures were established following standard procedures (Villegas and McPhaul 2005) and stored as frozen aliquots in liquid nitrogen. 6 fibroblast cell lines matched for sex, age and passage number were thawed out and grown to confluence in T75 culture flasks in standard culture media (DMEM containing 10% fetal bovine serum (FBS) and 1x Penicillin-Streptomycin).
Upon reaching confluence, 5x10^4 cells were plated per line into 13 different 6 well plates (1 well per line per plate). All 6 lines were collected in the same experiment for the RNA-seq experiment. Due to the labor-intensive nature of the ATAC protocol and the need to process cells fresh, the 6 lines were split into 2 batches, so 3 lines per batch were processed.

Assessment of Circadian Expression *in vitro*

In order to collect RNA or cells every 4 hours for 48 hours, cells were split into two batches, which were reset 12 hours apart (see schematic). Cells were reset 12 hours before the first collection to exclude the acute effects of dexamethasone and variation in synchronization conditions (Brown et al. 2005). 5 days after being plated the cells from batch one were synchronized by treatment with 100 nM Dexamethasone for 30 min. Cells were then washed with PBS and switched to collection media (DMEM containing 5% FBS and 1x Penicillin-Streptomycin). Lower concentration of FBS was used in this media to stop the cells from growing during the experiment, in order to keep all time points at approximately the same culture density. 12 hours later cells from batch 2 were synchronized and switched to collection media and the RNA/cell collection was started (from batch one).

RNA and Cell collection

For the collection of RNA, cells were lysed using 350uL RLT lysis buffer from the Qiagen RNeasy mini kit. Lysed cells were then scraped off the plate, transferred to a Qiaschredder (Qiagen 79656) and centrifuged for 2 min at max speed to further homogenize. Cell lysates were kept in -80 until extraction.

For the collection of cells for the ATAC protocol, cells were dissociated using 500uL of prewarmed TrypLE (ThermoFisher 12604013) and left for 5 min at 37℃. TrypLE was inactivated using 500uL of DMEM. Cells were then counted using the Logos Biosystems LUNA-FL automated cell counter, and 50x10^4 cells were used as input for tagmentation. Tagmented DNA for library preparation was collected following the previously described protocol (Buenrostro et al. 2015).

RNA extraction

RNA from cell lysates was extracted using the Qiagen RNeasy mini kit (Qiagen 74106). Cell lysates were extracted in a randomized order to prevent batch effects in downstream analysis. In order to collect total RNA including small RNAs, the standard extraction protocol (Purification of Total RNA from Animal Cells using Spin Technology) was adjusted by making the following changes:

- adding 1.5 volumes of 100% ethanol, instead of 70%, after the lysis step (step 4 in handbook protocol)
- Adding 700 mL of buffer RWT (Qiagen 1067933) instead of the provided RW1 (step 6 in handbook protocol)

RNA and ATAC sequencing

For the RNA sequencing, library preps were made using the Lexogen QuantSeq 3' mRNA-Seq Library Prep Kit and sequenced with 65-base single end reads, and sequenced at a targeted depth of 3.8M reads per sample, which is well above the recommended minimum 1M reads per sample read depth for these types of libraries.

ATAC seq libraries were generated following the previously described protocol (Buenrostro et al. 2015) and sequenced with 75-base double end reads, and sequenced at a targeted depth of 61M reads per sample.

Library preparation and sequencing was performed at the UCLA Neuroscience Genomics Core (https://www.semel.ucla.edu/ungc). All samples were sequenced on a Illumina HiSeq 4000 sequencer.

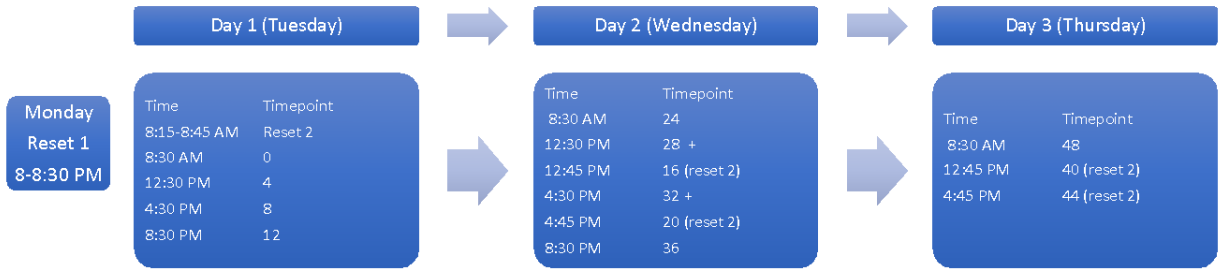

Schematic of synchronization and collection times

1. Villegas, J. McPhaul, M. Establishment and culture of human skin fibroblasts Curr. Protoc. Mol. Biol2005 Chapter 28, Unit 28.23

2. Brown, S. A., Fleury-Olela, F., Nagoshi, E., Hauser, C., Juge, C.,Meier, C. A., Chicheportiche, R., Dayer, J. M., Albrecht, U., and Schibler, U. (2005) The period length of fibroblast circadiangene expression varies widely among human individuals. PLoS Biol. 3, e338

RNA-seq data processing and analysis

Fastqc (Andrews, 2010) software was used to assess the quality of the read files. Low quality reads were trimmed using TrimGalore and Cutadapt.

Alignment of reads was performed with the STAR(Dobin et al. 2013) software and to human gene ensembl version GrCh38. STAR was indexed to the genome using the –runMode genomeGenerate function. For aligning, STAR was run with the parameters –outFilterType BySJout –outFilterMultimapNmax 20 –alignSJoverhangMin 8 –alignSJDBoverhangMin 1 –outFilterMismatchNmax 999 --outFilterMismatchNoverLmax 0.1 --alignIntronMin 20 --alignIntronMax 1000000 --alignMatesGapMax 1000000.

Samtools was used to index the aligned files from STAR.

Read counts were associated with genes using featureCounts software with the NCBI GRCh38 gene annotation file.

Analysis of the RNA-seq data used the R packages limma, Glimma and edgeR, as previously described (Law et al., 2018). Genes with low read counts were removed and reads were normalized by CPM. GeneIDs were converted to Gene Symbols using the package Homo.sapiens.

WGCNA (Langfelder and Horvath 2008) software was used to classify genes with similar temporal expression patterns. WGCNA was run using a power value of 12 obtained from diagnostic plots and with the "signed" argument. MetaScape was used for Gene Ontology analysis of the resulting gene sets from WGCNA.

Following the method described in (Mei et al. 2021), MetaCycle (Wu et al. 2016) was used to run circadian detection tools such as ARSER, JTK (Hughes, Hogenesch, and Kornacker 2010), LS and metacycle. In order to integrate results from the different individuals, the function meta3d was used from the Metacycle R package. RAIN (Thaben and Westermark 2014) was run separately.

Following the EdgeR use guide, cubic splines were generated using the splines package in R, with the ns function and 5 degrees of freedom. Resulting p-values were corrected using a false discovery rate of 0.05.

ATAC-seq data processing and analysis

Sequenced open chromatin data from the ATAC-seq assay followed the standard ENCODE Pipeline for the identification of open chromatin regions (OCRs) of the genome. The steps included using fastqc to evaluate the quality of the sequenced library. Followed by trimming of low quality reads with Trimgalore and Cutadapt. Alignment of the raw reads data to human gene Ensembl version GRCh38 was performed using bowtie2 (Langmead and Salzberg 2012) with a 2kb insert size and allowing up to 4 alignments. Reads within black-listed regions alongside PCR duplicates were removed with samtools. MACS2 (Y. Zhang et al. 2008) software was used to identify OCRs with parameters -g hs -q 0.01 –nomodel –shift -100 –extsize 200 –keep-dup all -B.

To compare the ATAC-seq signal across timepoints and subjects, we created a consensus bed file using the bedtools(Quinlan and Hall 2010) function merge function, combining all the overlapping peak regions across timepoints and subjects into a single file. The Featurecounts software was then used to assign read counts to those regions.

Read counts were normalized by RPM.

WGCNA (Langfelder and Horvath 2008) software was used to classify peaks with similar temporal accessibility patterns. WGCNA was run using a power value of 14 obtained from diagnostic plots and with the "signed" argument, identifying 15 modules.

HOMER (Heinz et al. 2010) findMotifsGenome.pllp program was used to identify enriched transcription factor motifs first individually in the peaks that belonged to the largest

WGCNA modules, as well as in the resulting set of grouping all the modules that displayed a similar increasing or decreasing pattern of accessibility.

Stratified linkage disequilibrium score regression analysis

Following the procedure described in (Ori et al. 2019), we applied an extension to sLDSR, a statistical method that partitions SNP-based heritability(h2) from GWAS summary statistics (Finucane et al. 2015). We ran sLDSR (ldsc.py –h2), using an ancestry-match 1000 Genomes Project phase 3 release reference panel, for each annotation of interest while accounting for the full baseline model, as recommended by the developers ((Finucane et al. 2015); (Gazal et al. 2017)), and an extra annotation of all the ATAC-seq detected in our in vitro model (n=3126 for peaks that were decreasing in accessibility, n=4415 for peaks increasing in accessibility), as well as extension of these regions by 1kb and 10kb genomic windows in both directions.

REFERENCES

Balsalobre, A., F. Damiola, and U. Schibler. 1998. “A Serum Shock Induces Circadian Gene Expression in Mammalian Tissue Culture Cells.” *Cell* 93 (6): 929–37.

Balsalobre, A., L. Marcacci, and U. Schibler. 2000. “Multiple Signaling Pathways Elicit Circadian Gene Expression in Cultured Rat-1 Fibroblasts.” *Current Biology: CB* 10 (20): 1291–94.

Berk, Maurice. 2018. “Smoothing-Splines Mixed-Effects Models in R Using the Sme Package: A Tutorial.” 2018. https://rdrr.io/cran/sme/f/inst/doc/Tutorial.pdf.

Bienvenu, O. J., D. S. Davydow, and K. S. Kendler. 2011. “Psychiatric ‘Diseases’ versus Behavioral Disorders and Degree of Genetic Influence.” *Psychological Medicine* 41 (1): 33–40.

Brown, Steven A., Fabienne Fleury-Olela, Emi Nagoshi, Conrad Hauser, Cristiana Juge, Christophe A. Meier, Rachel Chicheportiche, Jean-Michel Dayer, Urs Albrecht, and Ueli Schibler. 2005. “The Period Length of Fibroblast Circadian Gene Expression Varies Widely among Human Individuals.” *PLoS Biology* 3 (10): e338.

Buenrostro, Jason D., Beijing Wu, Howard Y. Chang, and William J. Greenleaf. 2015. “ATAC-Seq: A Method for Assaying Chromatin Accessibility Genome-Wide.” *Current Protocols in Molecular Biology / Edited by Frederick M. Ausubel ... [et Al.]* 109 (January): 21.29.1–21.29.9.

Chiou, Yi-Ying, Yanyan Yang, Naim Rashid, Rui Ye, Christopher P. Selby, and Aziz Sancar. 2016. “Mammalian Period Represses and de-Represses Transcription by Displacing CLOCK-BMAL1 from Promoters in a Cryptochrome-Dependent Manner.” *Proceedings of the National Academy of Sciences of the United States of America* 113 (41): E6072–79.

Demontis, Ditte, Raymond K. Walters, Joanna Martin, Manuel Mattheisen, Thomas D. Als, Esben Agerbo, Gísli Baldursson, et al. 2019. “Discovery of the First Genome-Wide Significant Risk Loci for Attention Deficit/hyperactivity Disorder.” *Nature Genetics* 51 (1): 63–75.

Dobin, Alexander, Carrie A. Davis, Felix Schlesinger, Jorg Drenkow, Chris Zaleski, Sonali Jha, Philippe Batut, Mark Chaisson, and Thomas R. Gingeras. 2013. “STAR: Ultrafast Universal RNA-Seq Aligner.” *Bioinformatics* 29 (1): 15–21.

Finucane, Hilary K., Brendan Bulik-Sullivan, Alexander Gusev, Gosia Trynka, Yakir Reshef, Po-Ru Loh, Verneri Anttila, et al. 2015. “Partitioning Heritability by Functional Annotation Using Genome-Wide Association Summary Statistics.” *Nature Genetics* 47 (11): 1228–35.

Fustin, J. M., J. S. O’Neill, M. H. Hastings, D. G. Hazlerigg, and H. Dardente. 2009. “Cry1 Circadian Phase in Vitro: Wrapped up with an E-Box.” *Journal of Biological Rhythms* 24 (1): 16–24.

Gazal, Steven, Hilary K. Finucane, Nicholas A. Furlotte, Po-Ru Loh, Pier Francesco Palamara, Xuanyao Liu, Armin Schoech, et al. 2017. “Linkage Disequilibrium-Dependent Architecture of Human Complex Traits Shows Action of Negative Selection.” *Nature Genetics* 49 (10): 1421–27.

Girshkin, Leah, Sandra L. Matheson, Alana M. Shepherd, and Melissa J. Green. 2014. “Morning Cortisol Levels in Schizophrenia and Bipolar Disorder: A Meta-Analysis.” *Psychoneuroendocrinology* 49 (November): 187–206.

Glynn, Earl F., Jie Chen, and Arcady R. Mushegian. 2006. “Detecting Periodic Patterns in Unevenly Spaced Gene Expression Time Series Using Lomb-Scargle Periodograms.” *Bioinformatics* 22 (3): 310–16.

Heinz, Sven, Christopher Benner, Nathanael Spann, Eric Bertolino, Yin C. Lin, Peter Laslo, Jason X. Cheng, Cornelis Murre, Harinder Singh, and Christopher K. Glass. 2010. “Simple Combinations of Lineage-Determining Transcription Factors Prime Cis-Regulatory Elements Required for Macrophage and B Cell Identities.” *Molecular Cell* 38 (4): 576–89.

Hida, A., Y. Ohsawa, S. Kitamura, K. Nakazaki, N. Ayabe, Y. Motomura, K. Matsui, et al. 2017. “Evaluation of Circadian Phenotypes Utilizing Fibroblasts from Patients with Circadian Rhythm Sleep Disorders.” *Translational Psychiatry* 7 (4): e1106.

Howard, David M., Mark J. Adams, Toni-Kim Clarke, Jonathan D. Hafferty, Jude Gibson, Masoud Shirali, Jonathan R. I. Coleman, et al. 2019. “Genome-Wide Meta-Analysis of Depression Identifies 102 Independent Variants and Highlights the Importance of the Prefrontal Brain Regions.” *Nature Neuroscience* 22 (3): 343–52.

Hughes, Michael E., John B. Hogenesch, and Karl Kornacker. 2010. “JTK_CYCLE: An Efficient Nonparametric Algorithm for Detecting Rhythmic Components in Genome-Scale Data Sets.” *Journal of Biological Rhythms* 25 (5): 372–80.

Iyer, Vishwanath R., Michael B. Eisen, Douglas T. Ross, Greg Schuler, Troy Moore, Jeffrey C. F. Lee, Jeffrey M. Trent, et al. 1999. “The Transcriptional Program in the Response of Human Fibroblasts to Serum.” *Science* 283 (5398): 83–87.

Jones, Samuel E., Jessica Tyrrell, Andrew R. Wood, Robin N. Beaumont, Katherine S. Ruth, Marcus A. Tuke, Hanieh Yaghootkar, et al. 2016. “Genome-Wide Association Analyses in 128,266 Individuals Identifies New Morningness and Sleep Duration Loci.” *PLoS Genetics* 12 (8): e1006125.

Keele, Gregory R., Bryan C. Quach, Jennifer W. Israel, Grace A. Chappell, Lauren Lewis, Alexias Safi, Jeremy M. Simon, et al. 2020. “Integrative QTL Analysis of Gene Expression and Chromatin Accessibility Identifies Multi-Tissue Patterns of Genetic Regulation.” *PLoS Genetics* 16 (1): e1008537.

Kripke, Daniel F., Caroline M. Nievergelt, Ej Joo, Tatyana Shekhtman, and John R. Kelsoe. 2009. “Circadian Polymorphisms Associated with Affective Disorders.” *Journal of Circadian Rhythms* 7 (January): 2.

Langfelder, Peter, and Steve Horvath. 2008. “WGCNA: An R Package for Weighted Correlation Network Analysis.” *BMC Bioinformatics* 9 (December): 559.

Langmead, Ben, and Steven L. Salzberg. 2012. “Fast Gapped-Read Alignment with Bowtie 2.” *Nature Methods* 9 (4): 357–59.

Leibenluft, E., P. S. Albert, N. E. Rosenthal, and T. A. Wehr. 1996. “Relationship between Sleep and Mood in Patients with Rapid-Cycling Bipolar Disorder.” *Psychiatry Research* 63 (2-3): 161–68.

Le Minh, N., F. Damiola, F. Tronche, G. Schütz, and U. Schibler. 2001. “Glucocorticoid Hormones Inhibit Food-Induced Phase-Shifting of Peripheral Circadian Oscillators.” *The EMBO Journal* 20 (24): 7128–36.

Levenson, Jessica, and Ellen Frank. 2011. “Sleep and Circadian Rhythm Abnormalities in the Pathophysiology of Bipolar Disorder.” *Current Topics in Behavioral Neurosciences* 5: 247–62.

Liu, Andrew C., Hien G. Tran, Eric E. Zhang, Aaron A. Priest, David K. Welsh, and Steve A. Kay. 2008. “Redundant Function of REV-ERBalpha and Beta and Non-Essential Role for Bmal1 Cycling in Transcriptional Regulation of Intracellular Circadian Rhythms.” *PLoS Genetics* 4 (2): e1000023.

Madden, Jamie M., Xia Li, Patricia M. Kearney, Kate Tilling, and Anthony P. Fitzgerald. 2017. “Exploring Diurnal Variation Using Piecewise Linear Splines: An Example Using Blood Pressure.” *Emerging Themes in Epidemiology* 14 (February): 1.

McCarthy, M. J., H. Wei, Z. Marnoy, R. M. Darvish, D. L. McPhie, B. M. Cohen, and D. K. Welsh. 2013. “Genetic and Clinical Factors Predict Lithium’s Effects on PER2 Gene Expression Rhythms in Cells from Bipolar Disorder Patients.” *Translational Psychiatry* 3 (October): e318.

Mei, Wenwen, Zhiwen Jiang, Yang Chen, Li Chen, Aziz Sancar, and Yuchao Jiang. 2021. “Genome-Wide Circadian Rhythm Detection Methods: Systematic Evaluations and Practical Guidelines.” *Briefings in Bioinformatics* 22 (3). https://doi.org/10.1093/bib/bbaa135.

Menet, Jerome S., Stefan Pescatore, and Michael Rosbash. 2014. “CLOCK:BMAL1 Is a Pioneer-like Transcription Factor.” *Genes & Development* 28 (1): 8–13.

Moreira, Ana Lúcia R., Anna Van Meter, Jacquelynne Genzlinger, and Eric A. Youngstrom. 2017. “Review and Meta-Analysis of Epidemiologic Studies of Adult Bipolar Disorder.” *The Journal of Clinical Psychiatry* 78 (9): e1259–69.

Mullins, Niamh, Andreas J. Forstner, Kevin S. O’Connell, Brandon Coombes, Jonathan R. I. Coleman, Zhen Qiao, Thomas D. Als, et al. 2021. “Genome-Wide Association Study of More than 40,000 Bipolar Disorder Cases Provides New Insights into the Underlying Biology.” *Nature Genetics* 53 (6): 817–29.

Nakahata, Yasukazu, Makoto Akashi, Daniel Trcka, Akio Yasuda, and Toru Takumi. 2006. “The in Vitro Real-Time Oscillation Monitoring System Identifies Potential Entrainment Factors for Circadian Clocks.” *BMC Molecular Biology* 7 (February): 5.

Nievergelt, Caroline M., Adam X. Maihofer, Torsten Klengel, Elizabeth G. Atkinson, Chia-Yen Chen, Karmel W. Choi, Jonathan R. I. Coleman, et al. 2019. “International Meta-Analysis of PTSD Genome-Wide Association Studies Identifies Sex- and Ancestry-Specific Genetic Risk Loci.” *Nature Communications* 10 (1): 4558.

Onat, O. Emre, M. Ece Kars, Şeref Gül, Kaya Bilguvar, Yiming Wu, Ayşe Özhan, Cihan Aydın, et al. 2020. “Human CRY1 Variants Associate with Attention Deficit/hyperactivity Disorder.” *The Journal of Clinical Investigation* 130 (7): 3885–3900.

Ori, Anil P. S., Merel H. M. Bot, Remco T. Molenhuis, Loes M. Olde Loohuis, and Roel A. Ophoff. 2019. “A Longitudinal Model of Human Neuronal Differentiation for Functional Investigation of Schizophrenia Polygenic Risk.” *Biological Psychiatry* 85 (7): 544–53.

Pizarro, Angel, Katharina Hayer, Nicholas F. Lahens, and John B. Hogenesch. 2013. “CircaDB: A Database of Mammalian Circadian Gene Expression Profiles.” *Nucleic Acids Research* 41 (Database issue): D1009–13.

Priest, James R., Kazutoyo Osoegawa, Nebil Mohammed, Vivek Nanda, Ramendra Kundu, Kathleen Schultz, Edward J. Lammer, et al. 2016. “De Novo and Rare Variants at Multiple Loci Support the Oligogenic Origins of Atrioventricular Septal Heart Defects.” *PLoS Genetics* 12 (4): e1005963.

Qin, Li, and Wensheng Guo. 2006. “Functional Mixed-Effects Model for Periodic Data.” *Biostatistics* 7 (2): 225–34.

Quinlan, Aaron R., and Ira M. Hall. 2010. “BEDTools: A Flexible Suite of Utilities for Comparing Genomic Features.” *Bioinformatics* 26 (6): 841–42.
Rijo-Ferreira, Filipa, and Joseph S. Takahashi. 2019. “Genomics of Circadian Rhythms in Health and Disease.” *Genome Medicine* 11 (1): 82.
Robles, Maria S., Sean J. Humphrey, and Matthias Mann. 2017. “Phosphorylation Is a Central Mechanism for Circadian Control of Metabolism and Physiology.” *Cell Metabolism* 25 (1): 118–27.
Saini, Camille, Jörg Morf, Markus Stratmann, Pascal Gos, and Ueli Schibler. 2012. “Simulated Body Temperature Rhythms Reveal the Phase-Shifting Behavior and Plasticity of Mammalian Circadian Oscillators.” *Genes & Development* 26 (6): 567–80.
Schibler, Ueli, and Paolo Sassone-Corsi. 2002. “A Web of Circadian Pacemakers.” *Cell* 111 (7): 919–22.
So, Alex Y-L, Teresita U. Bernal, Marlisa L. Pillsbury, Keith R. Yamamoto, and Brian J. Feldman. 2009. “Glucocorticoid Regulation of the Circadian Clock Modulates Glucose Homeostasis.” *Proceedings of the National Academy of Sciences of the United States of America* 106 (41): 17582–87.
Song, Jie, Sarah E. Bergen, Ralf Kuja-Halkola, Henrik Larsson, Mikael Landén, and Paul Lichtenstein. 2015. “Bipolar Disorder and Its Relation to Major Psychiatric Disorders: A Family-Based Study in the Swedish Population.” *Bipolar Disorders*. https://doi.org/10.1111/bdi.12242.
Stahl, Eli A., Gerome Breen, Andreas J. Forstner, Andrew McQuillin, Stephan Ripke, Vassily Trubetskoy, Manuel Mattheisen, et al. 2019. “Genome-Wide Association Study Identifies 30 Loci Associated with Bipolar Disorder.” *Nature Genetics* 51 (5): 793–803.
Thaben, Paul F., and Pål O. Westermark. 2014. “Detecting Rhythms in Time Series with RAIN.” *Journal of Biological Rhythms* 29 (6): 391–400.
Trubetskoy, Vassily, Antonio F. Pardiñas, Ting Qi, Georgia Panagiotaropoulou, Swapnil Awasthi, Tim B. Bigdeli, Julien Bryois, et al. 2022. “Mapping Genomic Loci Implicates Genes and Synaptic Biology in Schizophrenia.” *Nature* 604 (7906): 502–8.
Villegas, Jacob, and Michael McPhaul. 2005. “Establishment and Culture of Human Skin Fibroblasts.” *Current Protocols in Molecular Biology / Edited by Frederick M. Ausubel ... [et Al.]* Chapter 28 (August): Unit 28.3.
Walker, William H., 2nd, James C. Walton, A. Courtney DeVries, and Randy J. Nelson. 2020. “Circadian Rhythm Disruption and Mental Health.” *Translational Psychiatry* 10 (1): 28.
Wang, Yuedong, Chunlei Ke, and Morton B. Brown. 2003. “Shape-Invariant Modeling of Circadian Rhythms with Random Effects and Smoothing Spline ANOVA Decompositions.” *Biometrics* 59 (4): 804–12.
Wang, Zixi, Yaling Wu, Lanfen Li, and Xiao-Dong Su. 2013. “Intermolecular Recognition Revealed by the Complex Structure of Human CLOCK-BMAL1 Basic Helix-Loop-Helix Domains with E-Box DNA.” *Cell Research* 23 (2): 213–24.
Watanabe, Kyoko, Philip R. Jansen, Jeanne E. Savage, Priyanka Nandakumar, Xin Wang, 23andMe Research Team, David A. Hinds, et al. 2022. “Genome-Wide Meta-Analysis of Insomnia Prioritizes Genes Associated with Metabolic and Psychiatric Pathways.” *Nature Genetics* 54 (8): 1125–32.
Wu, Gang, Ron C. Anafi, Michael E. Hughes, Karl Kornacker, and John B. Hogenesch. 2016. “MetaCycle: An Integrated R Package to Evaluate Periodicity in Large Scale Data.” *Bioinformatics* 32 (21): 3351–53.
Yamazaki, Shin, and Joseph S. Takahashi. 2005. “Real-Time Luminescence Reporting of Circadian Gene Expression in Mammals.” *Methods in Enzymology* 393: 288–301.
Yan, Feng, David R. Powell, David J. Curtis, and Nicholas C. Wong. 2020. “From Reads to Insight: A Hitchhiker’s Guide to ATAC-Seq Data Analysis.” *Genome Biology* 21 (1): 22.
Yang, Rendong, and Zhen Su. 2010. “Analyzing Circadian Expression Data by Harmonic

Regression Based on Autoregressive Spectral Estimation." *Bioinformatics* 26 (12): i168–74.

Yang, S., H. P. A. Van Dongen, K. Wang, W. Berrettini, and M. Bućan. 2009. "Assessment of Circadian Function in Fibroblasts of Patients with Bipolar Disorder." *Molecular Psychiatry* 14 (2): 143–55.

Yu, Guangchuang, Li-Gen Wang, and Qing-Yu He. 2015. "ChIPseeker: An R/Bioconductor Package for ChIP Peak Annotation, Comparison and Visualization." *Bioinformatics* 31 (14): 2382–83.

Zhang, Luoying, Arisa Hirano, Pei-Ken Hsu, Christopher R. Jones, Noriaki Sakai, Masashi Okuro, Thomas McMahon, et al. 2016. "A PERIOD3 Variant Causes a Circadian Phenotype and Is Associated with a Seasonal Mood Trait." *Proceedings of the National Academy of Sciences of the United States of America* 113 (11): E1536–44.

Zhang, Ray, Nicholas F. Lahens, Heather I. Ballance, Michael E. Hughes, and John B. Hogenesch. 2014. "A Circadian Gene Expression Atlas in Mammals: Implications for Biology and Medicine." *Proceedings of the National Academy of Sciences of the United States of America* 111 (45): 16219–24.

Zhang, Yong, Tao Liu, Clifford A. Meyer, Jérôme Eeckhoute, David S. Johnson, Bradley E. Bernstein, Chad Nusbaum, et al. 2008. "Model-Based Analysis of ChIP-Seq (MACS)." *Genome Biology* 9 (9): R137.

Zhou, Yingyao, Bin Zhou, Lars Pache, Max Chang, Alireza Hadj Khodabakhshi, Olga Tanaseichuk, Christopher Benner, and Sumit K. Chanda. 2019. "Metascape Provides a Biologist-Oriented Resource for the Analysis of Systems-Level Datasets." *Nature Communications* 10 (1): 1523.